JOURNAL OF SPACECRAFT AND ROCKETS
Vol. 38, No. 5, September–October 2001

Fast-Response Heat-Flux Sensor for Measurement Commonality in Hypersonic Wind Tunnels

Carl T. Kidd* and John C. Adams Jr.†
Sverdrup Technology, Inc., Arnold Air Force Base, Tennessee 37389

A fast-response heat-flux sensor, based on a modified Schmidt–Boelter gauge principle of operation, has been developed for commonality of heat transfer measurement methodologies in Arnold Engineering Development Center hypersonic wind tunnels. This sensor retains the direct-reading and self-generating high-output capabilities of the traditional Schmidt–Boelter gauge, but a novel fabrication feature provides near first-order exponential time response with time constants in the 10–15-ms range. This transducer can be used in blowdown wind tunnels as well as quasi-steady-state measurement applications. Coupled with recent developments in data correction and time-response algorithms, the development of this direct-reading sensor has significantly improved the accuracy and versatility of heat-flux measurements in hypersonic testing applications. Gauge design features, laboratory performance characterization, generalized algorithm development, and hypersonic wind-tunnel data comparisons are presented.

Nomenclature

$d\dot{q}/dt$	=	derivative of heat flux with respect to time, Btu/(ft^2 · s)/s
E_0	=	gauge output signal, mV
g	=	response function
K	=	thermal conductivity, Btu/(ft · s · °F)
L	=	sharp cone length, ft
ℓ	=	thickness of thermal resistance layer, in.
N	=	number of turns of wire on thermopile coil
n	=	exponent in quasi-first-order gauge response function
Pinf	=	freestream pressure, psia
Qinf	=	dynamic pressure, psia
$\dot{q}$	=	heat flux or heat-transfer rate, Btu/(ft^2 · s)
rho	=	freestream density, lb/ft^3
SF	=	gauge scale factor, Btu/(ft^2 · s)/mV
T	=	temperature, °F or °R
Tinf	=	freestream temperature, °R
t	=	time, s
Uinf	=	freestream velocity, ft/s
x	=	distance along aerodynamic length, ft
α	=	angle of attack, deg
Γ	=	gamma function
Δ	=	difference
σ	=	relative Seebeck coefficient of the series combination of thermoelements, mV/°F
τ	=	gauge time constant, s
τ^*	=	characteristic time measure of the integrated energy deficiency in the gauge response, s

Subscripts

C	=	cold junction
corr	=	corrected value of parameter
H	=	hot junction
ind	=	indicated value of parameter
input	=	input condition
meas	=	measured value of parameter
s	=	measurement along surface of sharp cone configuration

Presented as Paper 2000-2514 at the AIAA 21st Aerodynamic Measurement Technology and Ground Testing Conference, Denver, CO, 19–22 June 2000; received 10 August 2000; revision received 17 May 2001; accepted for publication 19 May 2001.

*Senior Engineer, Aircraft Systems Test and Evaluation Department, Small Aeronautical Systems Branch, Arnold Engineering Development Center, 675 Second Street; carl.kidd@arnold.af.mil.

†Technical Principal: Hypersonics, Office of General Manager, Arnold Engineering Development Center, 676 Second Street; jcadams@arnold.af.mil. Associate Fellow AIAA.

Introduction

TRANSIENT heat transfer in hypersonic flow ground-test facilities is normally measured with surface temperature sensing devices, and the time-resolved data are then processed to calculate heat-flux parameters with an inverse numerical equation.[1,2] The appropriate application of such an equation requires the assumption of one-dimensional, semi-infinite solid heat conduction. Examples of transient surface temperature sensors are the coaxial surface thermocouple,[3–5] thin-film resistance thermometer,[6,7] null-point calorimeter,[8,9] and thermographic phosphor.[10] All of these devices or methods have significant deficiencies that can contribute to degradation of the accuracy of the measurement. Heat storage methods such as the thin-skin thermocouple technique[11,12] and the slug calorimeter[13] also have limitations in transient measurement applications.

Conversely, the prominent direct-reading heat-flux transducers such as the Gardon gauge[14] (also see Ref. 15) and the Schmidt–Boelter gauge (see Refs. 16 and 17) are traditionally regarded as quasi-steady-state sensors and are often not given proper consideration in transient measurement applications. It is recognized that these direct-reading sensors can be experimentally calibrated to high accuracy (≤3% bias uncertainty) using heat-flux standards certified by the National Institute of Standards and Technology (NIST). Direct-reading sensors such as the Schmidt–Boelter gauge are effective in some transient applications and possess the added feature of being able to transition into the steady-state test regime where surface temperature sensors cannot be used.[18]

A heat-flux sensor development study was recently conducted at the Arnold Engineering Development Center (AEDC) to investigate the use of direct-reading sensors in transient applications. The primary reason for this effort is that significant test cost savings can be achieved if test articles can be swept in the pitch and/or roll mode to obtain data at several angles of attack for a given tunnel run. It is standard procedure for the AEDC high-Mach-number Tunnel 9 facility to operate in the continuous pitch mode. Development of direct-reading sensors with fast response capabilities will result in a commonality of test measurement methodology, where test articles can be used interchangeably between the AEDC Tunnel 9 facility, located at White Oak, Maryland, and the AEDC Hypersonic Wind Tunnels B and C, located at Arnold Air Force Base, Tennessee. The current study involved modeling the measurement device with state-of-the-art, finite element analysis (FEA) software to test all types of transient heat-flux input. Although the Gardon gauge is simpler to model analytically, the Schmidt–Boelter gauge

offers several operational advantages and is the sensor of choice in this measurement application. This analytical study led to the practical implementation of an innovative method of fabricating miniature (0.062–0.125-in.-diam) Schmidt–Boelter gauges to achieve fast time response, near first-order exponential time response, and high output.

Development of fast-response Schmidt–Boelter gauges does not mean that these sensors can operate in the steady-state mode in transient heat-transfer environments such as those experienced in Tunnel 9. There are restrictions on the use of direct-reading sensors in highly transient environments, and these limitations are defined in the present work. It is implied that the basic thermal response of the direct-reading gauges can be accurately described by the measured response of the gauge to a step input in heat flux. This behavior can be analytically estimated and verified by laboratory procedures. A consistent, nonambiguous data reduction methodology for fast-response Schmidt–Boelter gauges, which is easy to implement in an algorithmic format, was recently developed at the AEDC.[19] Time-wise correction of measured Schmidt–Boelter gauge heat flux is no more difficult than that involved in a classical first-order system and involves only the determination of a characteristic time measure of the integrated energy deficiency inherent in the gauge response. This characteristic time measure is easily determined from the gauge response characterization to a step input heat flux by numerical integration of the response-vs-time data. The correction equation applies to sensors with time-response characteristics that exhibit less than first-order response.

The design and development of the new fast-response Schmidt–Boelter gauge, its experimental characterization with the new data reduction methodology, and the correction equation used in typical hypersonic wind-tunnel transient heat transfer measurement applications are discussed. Approximately 200 of the new gauges were fabricated and installed in a scale model of a complex test article for an aerothermal test program conducted in Tunnel B at Mach numbers 6 and 8 during December 1999. Approximately 200 wind-tunnel runs were conducted in that test program.

Description of Wind-Tunnel Facilities

Tunnels B and C

AEDC Hypersonic Wind Tunnels B and C are large, closed-circuit, continuous-flow, high-productivity, variable-density wind tunnels with 50-in.-diam test sections. Axisymmetric contoured nozzles provide freestream Mach numbers of 6 and 8 in Tunnel B and 10 in Tunnel C. Stagnation temperatures up to 1440°F are obtained through the use of natural-gas-fired combustion heaters in series with an electric resistance heater. The test article mounting system has the capability of positioning a 1000-lb model through ±15 deg in pitch and ±180 deg in roll. The maximum continuous sweep rates in Tunnels B and C are 3 and 1 deg/s, respectively. These tunnels are equipped with a model injection system that permits removal while the tunnel remains in operation. The injection system permits precision control of model flow immersion time and model wall initial conditions. An additional advantage of the injection system is model accessibility for rapid configuration changes while the tunnel is in continuous operation. The injection tank, where the model is located when retracted from the test flow, also contains an air-cooling system to assist in controlling model wall initial conditions for the subsequent run.

Tunnel 9

AEDC Tunnel 9 is the primary high-Mach-number, high-Reynolds-number facility for aerodynamic testing in the United States.[20] The tunnel is a blowdown facility that currently operates at Mach numbers 7, 8, 10, 14, and 16.5. Pure nitrogen is used as the working fluid, and unique hardware exists to provide maximum temperatures of 3,000°F and pressures of 20,000 psia. Long, contoured, axisymmetric nozzles expand the high-temperature and pressure supply to a 5-ft-diam test section while providing a uniform flow ideal for aerodynamic testing. The test article mounting system, also unique to Tunnel 9, is capable of pitching a 200-lb model through 40 deg at rates up to 80 deg/s, maximizing the data collection during the useful run time.

Schmidt–Boelter Gauge Principle of Operation

The principle of operation of the Schmidt–Boelter gauge can be divided into two distinctly different performance categories. These are the thermal and thermoelectric functions. There are valid reasons for separating the two for a complete understanding of gauge operation. Both the thermal and the thermoelectric functions are described completely in Ref. 17 for a gauge operating in the quasi-steady-state mode. Because the present paper primarily describes transient measurements, the steady-state explanation of the thermal function of the gauge is insufficient for transient applications. However, the thermoelectric function described in Ref. 17 is the same for any Schmidt–Boelter gauge, and the steady-state thermal function is helpful for understanding basic gauge concepts.

The Schmidt–Boelter gauge concept is adequately represented by Fig. 1. From a thermal perspective, the gauge operates on the principle of axial heat conduction. It will be shown that for a constant surface heat flux $\dot{q}$ a constant temperature difference ΔT is developed between the top and bottom surfaces of an electrically insulating wafer, often referred to as the thermal resistance layer.[21] The wafer is supported at both ends by a high thermal conductivity gauge body material, which also serves as the heat sink. This temperature ΔT is a measurement of the difference between temperatures at the top surface T_H and the bottom surface T_C of the wafer. A differential thermocouple measuring this temperature difference will have an output signal E_0, which is proportional to the input heat flux $\dot{q}$. The thermoelectric function of the gauge is achieved by winding a small-diameter bare constantan wire around a wafer of an electrically insulating material. One-half of the wire/wafer assembly is then electroplated with a material that is thermoelectrically compatible with constantan thermocouple wire. Boelter used silver as the plating material in his initial gauge, but most manufacturers now use copper. This electrical configuration creates a series connection of the plated copper on constantan and constantan differential thermocouples with the hot junctions at a temperature T_H on the top surface of the wafer and the cold junctions at a temperature T_C on the bottom surface. This series combination of differential thermocouples is a thermopile. The relative Seebeck coefficient σ of this parallel combination of thermoelements is slightly less than the

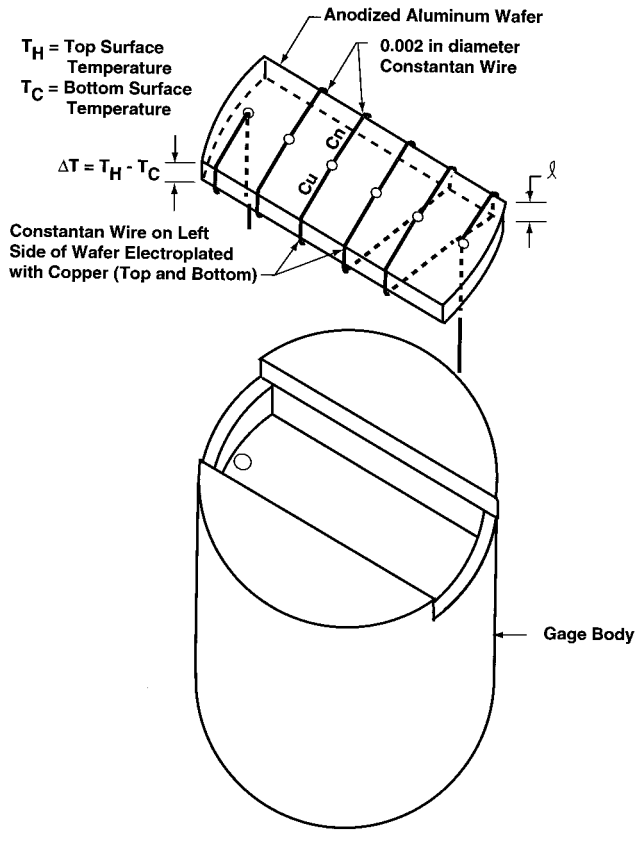

Fig. 1 Schmidt–Boelter gauge concept.

actual combination of copper with constantan.[17] The output signal can be represented by

$$E_0 = N\sigma(T_H - T_C) \quad (1)$$

where N is the number of turns of constantan wire around the wafer and σ is the relative Seebeck coefficient of the series combination of thermoelements. This description provides a simplified explanation of the gauge concept for steady-state applications.

Although Fig. 1 is useful for introduction of principles of operation purposes, most actual gauges are composed of several different materials due to the specific requirements of the applications for which they are intended. The thermal model of the actual gauge can be much different from the simple model. The thermal model defines heat conduction paths within gauge components from which the axial temperature gradients between parallel plane surfaces in the gauge are measured. These axial temperature gradients are the principal gauge heat-flux measurement mechanism. Gauge materials, position of parallel plane surfaces, and axial distance between plane surfaces all affect the time-response characteristics and output of the gauge. Because of its rather complex geometrical configuration, multiple-material composition, and numerous heat conduction paths, the Schmidt–Boelter gauge used in typical aerospace applications cannot be analyzed using common analytical methods. Therefore, another method is needed to accurately predict gauge behavior. The method used most successfully at the AEDC is FEA, a heat conduction code with capabilities to 1) model the gauge in three dimensions, 2) permit the introduction of many different materials, and 3) accept general transient heat transfer inputs. The MSC/NASTRAN™ for Windows version 3.0 software package[22] has such capabilities and has provided accurate analysis of steady-state and transient gauge behavior for design purposes.

Designing Heat-Flux Sensors with FEA

Designing transducers to measure aerodynamic parameters such as force and moment and, in some cases, pressure, is rather straightforward when using FEA methods. Heat transfer measurement methods such as the Gardon gauge[14] (also see Ref. 15) and the thin-skin technique[11] can be reduced to one- or two-component systems and be confidently designed using FEA. However, the Schmidt–Boelter gauge is typically a multimaterial system and becomes somewhat more difficult to design with FEA. It can be stated with confidence that FEA methods may be effectively used to refine Schmidt–Boelter gauge designs, if not used completely during the design. A set of step-by-step instructions was used to perform the Schmidt–Boelter gauge design for fast-response measurement applications in AEDC Wind Tunnel 9 (Ref. 18). One aspect of the analytical model that is important to designing with FEA is the calibration of the numerical model with a step heat-flux input. This calibration is subsequently used when highly transient heat-flux inputs to the analytical model are applied and studied.

Construction of the FEA Model

FEAs of the Schmidt–Boelter gauge concept were performed to gain knowledge and understanding of gauge performance criteria in the transient mode of operation. Efforts were made to use actual physical dimensions and materials of gauges specifically designed for fast-response or transient operation in the construction of the finite element model. The overall dimensions of the gauge considered are 0.125 in. (diameter) by 0.125 in. (length). These dimensions are the same for the majority of actual gauges constructed at the AEDC. The computer-generated scale drawing of the finite element model shown in Fig. 2a was constructed to represent the actual gauge design. All finite elements and nodal points are shown in this wire frame depiction. The MSC/NASTRAN program maintains the proper relative dimensional scales on drawings in each of the three planes of reference. Because the actual gauge is effectively a cylinder, the FEA model can be accurately represented by an axisymmetric geometry. Therefore, depictions are shown in two dimensions.

Description of the FEA model

The model shown in Fig. 2a was constructed of 400 finite elements and 231 nodal points and consists of three main parts: 1) the thermal resistance layer, 2) the filler layer, and 3) the gauge body or heat sink. The majority of the finite elements are concentrated in the thermal resistance layer. Although the thermal resistance layer is but a fraction of the thermal mass of the gauge, it is in this section of the gauge that the temperature differences, which are so significant to both the output and time response of the gauge, are generated. Therefore, the majority (280) of the finite elements are concentrated in this part of the model. The remainder of the finite elements are located in the filler layer just below the thermal resistance layer and in the aluminum heat sink. It will be shown that the material in the filler layer is vital to the proper operation of the gauge. For the expanded and solid shaded element FEA model shown in Fig. 2b, a specified heat flux (denoted as diamonds with stems) was considered on the top (sensing) surface of the gauge. All other outside surfaces were considered adiabatic (no heat flow). Results of the FEA analyses show how gauge operating characteristics can be affected by parametrically changing gauge materials and altering certain gauge dimensions. These analyses are intended to help the gauge designer achieve desired operating characteristics with actual gauges.

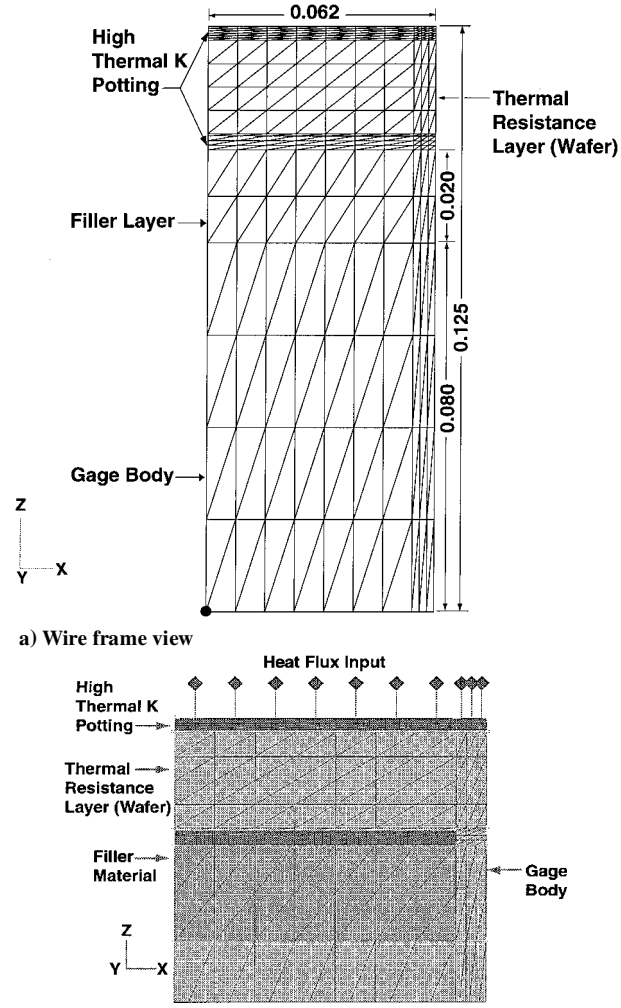

Fig. 2 Schmidt–Boelter gauge FEA model.

Data Reduction Methodology

Fast-response Schmidt–Boelter gauges often have time-response characteristics that are not first-order exponential. The sensor design presented describes a gauge whose time-response characteristics are usually near first-order exponential. However, first generation AEDC fast-response gauges[18] and gauges from other manufacturers have exponential time responses whose order can vary between 0.60 and 1.0. To ensure accurate data reduction in impulse facilities such as AEDC Tunnel 9, a correction term must be added to the measured heat flux, whose magnitude is dependent on the time

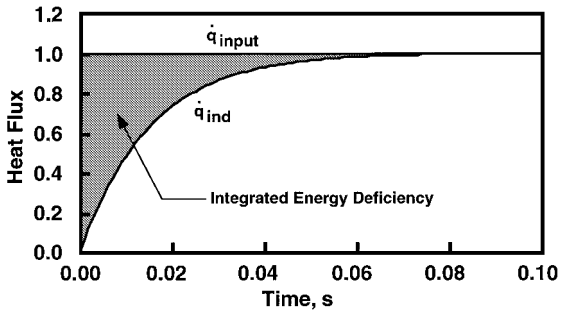

Fig. 3 Typical Schmidt–Boelter gauge response to step input in heat flux.

constant of the gauge and the exponential order of the gauge's time response. The time-response characteristics of every manufactured gauge should be evaluated in the laboratory before the gauge is used in any transient heat transfer measurement applications. A general data reduction methodology that is suitable for non-first-order systems is required.

In 1997 Hudson[23] derived such an equation, and it was used in reduction of data from first-generation AEDC fast-response Schmidt–Boelter gauges. However, it was observed that Hudson's equation required excessive computer storage for rapid calculations. A new methodology, which is easier to implement, was developed at the AEDC,[19] and only the newer methodology is reviewed in this work. The new method has proved to be a very accurate and efficient method of obtaining data from fast-response Schmidt–Boelter gauges, has proven extremely useful in the laboratory experimental characterization of gauge time response, and can be implemented in a simple and cost-effective manner.

The approach of the new data reduction methodology is based on interpretation of the integrated energy deficiency of the gauge in response to a step input in heat flux. With reference to Fig. 3, which shows a typical step input response curve, the energy deficiency inherent in the gauge response at any point in time is defined as $(\dot{q}_{input} - \dot{q}_{ind})$. Performing the time integral yields

integrated energy deficiency in gauge

$$= \int_0^\infty (\dot{q}_{input} - \dot{q}_{meas})\,dt = \dot{q}_{input}\tau^* \tag{2}$$

where τ^* is a characteristic time measure of the integrated energy efficiency inherent in the gauge response. (This energy efficiency is illustrated by the shaded area in Fig. 3.) Defining the gauge response function $g(t)$ as

$$g(t) = \dot{q}_{meas}/\dot{q}_{input} \tag{3}$$

results in

$$\tau^* = \int_0^\infty [1 - g(t)]\,dt \tag{4}$$

which yields $\tau^* \equiv \tau$ for the special case of classical first-order system response:

$$g(t) = 1 - \exp(-t/\tau) \tag{5}$$

One can then consider the quasi-first-order system response, defined by the function proposed in Ref. 18, as appropriate for fast-response Schmidt–Boelter gauges, namely

$$g(t) = 1 - \exp(-t/\tau)^n \tag{6}$$

where n is a constant typically less than unity. The response time τ is determined as the time in which

$$g(t = \tau) = 1 - \exp(-1) = 0.632 \tag{7}$$

which is totally independent of the value of n. With τ determined in this (classical) manner, the proper value of n is given by the definition of

$$\tau^* = \int_0^\infty [1 - g(t)]\,dt = \int_0^\infty \exp\left[\left(\frac{-t}{\tau}\right)^n\right] dt \tag{8}$$

which does not have a closed-form integral solution. Thus, for a value of τ^* defined by numerical integration of the gauge response function $g(t) = \dot{q}_{meas}/\dot{q}_{input}$, it is necessary to vary the value of n via a Newton–Raphson iteration procedure until the correct value of τ^* is obtained.

Data reduction of unsteady heat transfer may be accomplished by application of the correction to the measured heat flux:

$$\dot{q}_{corr} = \dot{q}_{meas} + \tau^*\left(\frac{d\dot{q}_{meas}}{dt}\right) \tag{9}$$

This method has been successful with transducers such as the Gardon gauge, which has a first-order transient response ($\tau^* = \tau$). Note that the only requirement in its application is the value of τ^*, which is based on a numerical integration of the empirical gauge response curve to a step input heat flux; one does not have to fit the gauge response curve with the τ and n parameters. A general method of selecting the proper fast-response Schmidt–Boelter gauge response time for a given application is presented in the Appendix.

Application of Data Reduction Methodology

The data reduction methodology described involving τ^* has been applied to an FEA model of the Schmidt–Boelter gauge to determine the characteristic timewise parameters of the model. These timewise parameters were then used in the reduction of heat transfer data when input from an actual hypersonic wind-tunnel test run is applied to the same FEA model.

Calibration of FEA Model

One of the first steps in Schmidt–Boelter gauge design with FEA is calibration of the analytical model with a step input heat flux. Figure 4 shows the calculated time-response parameters n, τ, and τ^* associated with an analytical model whose exponential order of time response is significantly less than unity, that is, $n < 1$. These parameters were determined by applying a step function heat flux to the sensing surface and measuring the simulated transient gauge output (actually the temperature difference between two selected nodal points). Note that n has a value of 0.807, which is typical of a Schmidt–Boelter gauge of conventional design. In addition, the value of τ^* (0.0156 s) is about 13% greater than the value of τ (0.0138 s). This difference is also typical of a gauge whose order of exponential time response is significantly less than unity.

Application with Experimental Data

The primary application for fast-response Schmidt–Boelter gauges at the AEDC is in transient heat transfer measurements on an aerodynamic model configuration in a hypersonic wind tunnel. The accuracy of the data reduction methodology is demonstrated by using actual wind-tunnel data as input to the FEA model. The most severe transient conditions at the AEDC are experienced in the Tunnel 9 facility at White Oak, Maryland. A tunnel run at freestream Mach number 10, nominal freestream Reynolds number 20×10^6/ft, total run duration of 0.30 s, and average pitch rate (APR) of 62 deg/s was selected to test the data reduction methodology as applied to the FEA model. The heat-flux input to the FEA model was obtained

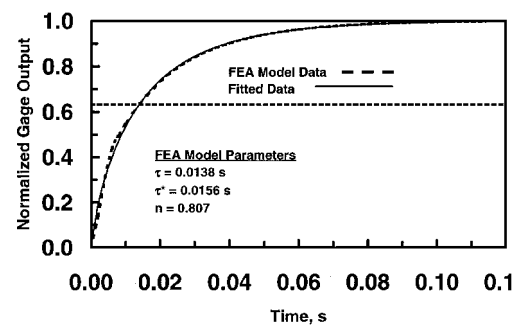

Fig. 4 Time-response calibration data for an FEA Schmidt–Boelter gauge model.

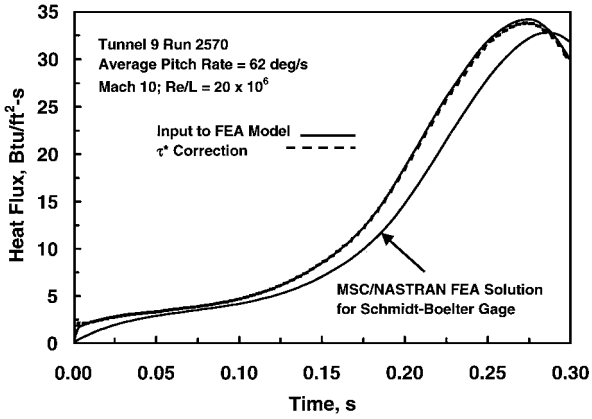

Fig. 5 Transient heat-flux data reduction using Schmidt–Boelter gauge FEA model.

from heat-flux data measured by a coaxial surface thermocouple mounted on a large, spherically blunted cone (Tunnel 9 run 2570). This input, shown in Fig. 5, was applied to the sensing surface of the FEA model. The indicated timewise heat-flux solution shown represents what an actual Schmidt–Boelter gauge would measure before the data are corrected for time lag effects. As can be seen from Fig. 5, the indicated heat flux lags the input heat flux by a substantial amount (10–25%) during most of the 0.30-s run duration. Corrected data are obtained by the use of Eq. (9) and involve the time derivative of the indicated heat flux multiplied by the τ^* parameter and added to the indicated heat flux at each time point. Application of the τ^* correction methodology to this transient condition results in almost perfect agreement between the input and the corrected heat flux as shown in Fig. 5.

Schmidt–Boelter Gauge Design Concepts

Before 1999, Schmidt–Boelter gauges at the AEDC had always been fabricated by what is referred to as the conventional method. The sensor concept consisted of a wafer or thermal resistance layer backed by a heat sink of high thermal conductivity material, such as copper or aluminum. The output-producing mechanism of the gauge depends on a coil of small (0.001- or 0.002-in.-diam) constantan wire wound around an electrically insulating wafer. The bare wires are electroplated with copper over one-half of the wafer, top and bottom, to form a thermopile. The wires are protected and electrically insulated by a thin layer of high thermal conductivity epoxy. Therefore, the wafer was separated from the heat sink by this epoxy layer on the bottom and sides of the wafer. The term heat sink is a misnomer in this application because the so-called heat sink actually serves as a body or support for the gauge and provides less than perfect heat sinking for the thermal resistance layer. However, gauges of this type performed satisfactorily in the AEDC continuous wind tunnels, as long as the gauges were fabricated with tightly wound coils and the thermal conductivity of the epoxy was relatively high. Initial efforts to make fast-response gauges concentrated on making the wafer thin, the constantan wires small, winding the coils tightly, and using thin layers of high thermal conductivity epoxy.

Gauges of this type were fabricated at the AEDC and other places and are reported in Ref. 18. Although these gauges had time constants in the range of 10–15 ms, there were several disadvantages associated with this design. First, the order n of the exponential time response of the gauges was significantly less than unity, typically being 0.60–0.80. Another problem with these gauges was that fabrication was difficult because the effort to achieve fast time response required use of thinner wafers, smaller constantan wires, and thin, tightly packed epoxy layers. Although it was possible to achieve fast response with gauges of conventional design, the relative cost had increased, and special care had to be given in the characterization of the time response.

Efforts were initiated under an AEDC technology project in 1999 to design a gauge with near first-order response using simpler fabrication procedures. This design and analysis was performed with the aid of FEA of the gauge concept. Because it is fairly simple

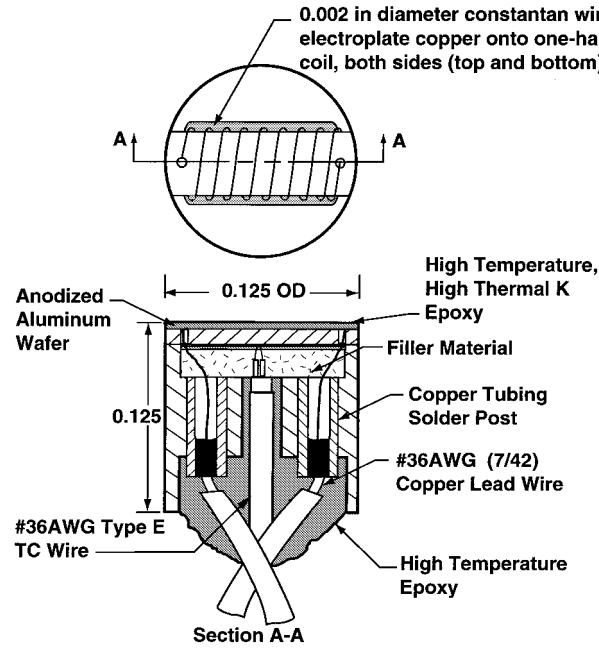

Fig. 6 Half-section of Schmidt–Boelter gauge.

to change geometry and materials with FEA, several combinations were tried. One concept studied was to heat sink the wafer by allowing it to extend to the edge of the gauge body. Perfect thermal contact with the gauge body on both ends of the rectangular wafer was assumed. This feature decreased the time constant of the gauge and also increased the exponential order of the simulated gauge output. In addition, other design changes were implemented. It soon became apparent that the thermal conductivity of the filler material immediately behind the wafer was a significant factor in gauge performance. Different filler materials were considered. Results of FEA showed that first-order time response could be achieved with a filler material of low thermal conductivity. This combination of minor design changes resulted in the design of a gauge that had 1) near first-order time response, 2) simpler fabrication procedures, and 3) lower cost of fabrication. However, there is at least one negative aspect of this modified Schmidt–Boelter gauge: the output was decreased by approximately 50%. Ultimately, the gauge designer must balance choice of materials and gauge dimensions to have sufficiently fast time response and adequate gauge output for the intended application.

Figure 6 shows a cross-section of the AEDC Schmidt–Boelter gauge described, which can be used interchangeably in AEDC Hypersonic Tunnels B and C and Tunnel 9. The gauge has a 0.125-in. diam and a 0.125-in. length. Gauge length can be extended to simplify fabrication procedures and can be shortened somewhat to fit in thin model walls. The gauge has a sensitivity of about 0.5 mV/(Btu/ft^2 · s) and a first-order time constant in the 10–15-ms range. The gauge can be contoured in the cross-axis plane to around a 0.10-in. radius of curvature. The gauge has a maximum service temperature of around 600°F.

Laboratory Calibration, Time Response, and Performance Testing

Calibration

Schmidt–Boelter gauges were calibrated in the AEDC Aerothermodynamics Measurements Laboratory (ATMLab). The heat source used was a nine-unit 1-kW tungsten filament lamp bank, which provides uniform heat flux varying from 0.5 to 10 Btu/(ft^2 · s) over a surface area measuring 4 × 1.5 in. (Ref. 24). Outputs from up to 24 sensors are routed to instrumentation amplifiers. These amplifiers provide gain of up to 15,000 and analog filtering. Amplifier outputs are routed to the inputs of a 32-channel, 16-bit analog-to-digital converter. A calibration through the data system using a NIST traceable millivolt standard is performed at the beginning of each day the system is used. It has been determined by statistical analysis that the

data system adds an uncertainty of ±0.5% to the experimental calibrations. Up to 19 gauges can be calibrated simultaneously against three heat-flux standard 0.187-in.-diam Schmidt–Boelter standard gauges calibrated at the NIST Optical Technology Division Physics Laboratory and certified to be accurate to ±2.0% deviation over a range of heat flux up to 8.8 Btu/(ft^2 · s). A group of three transfer standard gauges is used over a time period up to 12 months and is replaced with another group of gauges calibrated by NIST in the same manner. Experimental procedures followed by NIST in the calibration of the transfer standard gauges are documented.[25] The calibration heat-flux level is determined by taking the average of the indicated heat flux from the three transfer standard gauges over a common time interval. Measured heat flux from the three transfer standard gauges is normally within 1% deviation. The output from each of the test gauges is measured over the same time interval over which the individual outputs of the transfer standard gauges are measured. The calibration scale factor [Btu/(ft^2 · s)/mV] for each gauge is calculated by a straight-line fit through three data points obtained at three different heat-flux levels, plus zero (no heat flow). These calibrations are performed under the control of graphical programming software, and results are available in tabular and/or plotted format.

Time-Response Measurements

Time-response characteristics of Schmidt–Boelter gauges are experimentally obtained with the same data acquisition system. The system was configured to sample output signals from only two analog channels (at 5000 samples/s) to focus a higher heat flux onto one gauge at a time and mechanically shutter the heat source during the initial part of the experimental procedure. The heat source has a 200-W tungsten filament lamp with an ellipsoidal reflector.[8] This device is capable of delivering up to 75 Btu/(ft^2 · s) onto a 0.30-in.-diam focal spot and has proved to be quite useful in the ATMLab for special radiant heating applications.

The actual Schmidt–Boelter gauge time-response experimental procedures are relatively straightforward. The gauge is placed directly under the heat source at a distance of about 1 in. A high absorptivity coating on the gauge front surface used for the heat-flux calibrations is removed before the time-response checks. The data system and an electronically controlled, mechanically operated fast shutter are initiated simultaneously, allowing the gauge to be irradiated by the heat source at a time point approximately 50 ms from the start of data acquisition. The data system is set at a nominal sampling rate of 5000 samples/s, and approximately 2500 samples are acquired. The gauge output raw data are viewed on a timewise plot to determine the gauge suitability for fast-response measurement applications. The gauge output data are then written to a database, where the data are normalized to the steady-state output. The normalized data are also adjusted in time to the beginning of gauge heating. A very useful application of the database is to provide a timewise plot of the measured and fitted data along with the calculated n, τ, and τ^* parameters for the gauge.

Normalized experimental time-response data from an AEDC 0.125-in.-diam Schmidt–Boelter gauge are shown in Fig. 7. The time-response parameters τ, τ^*, and n calculated using the new data reduction methodology are shown on the graph. Good agreement of the experimental data (dashed line) with the fitted data (solid line) is observed. Also note that the value of the calculated exponential order n of the time-response curve is quite close to 1.0. A horizontal dashed line representing 63.2% of full-scale output is shown on the graph to represent the classical first-order time constant. Note that the experimental data and the fitted data coincide at the time point τ, where they cross the 63.2% line. That the time-response parameters τ and τ^* agree very closely provides confidence that an accurate timewise correction can be applied to transient data obtained with this gauge. The gauge time response shown in Fig. 7 is typical of over 200 of these gauges that were fabricated for an aerothermal test program on a scale model of a complex hypersonic flight vehicle tested in AEDC Wind Tunnel B in December 1999.

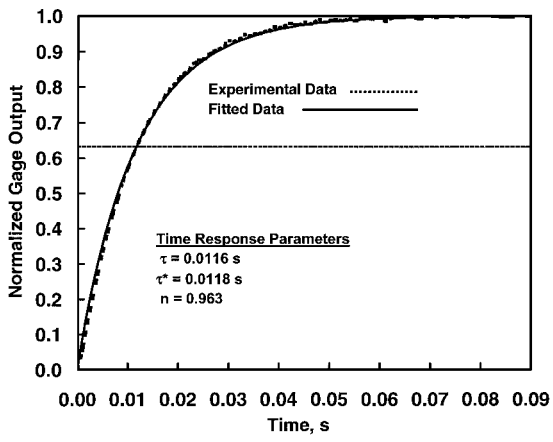

Fig. 7 Experimental time response of Schmidt–Boelter gauge with fitted data.

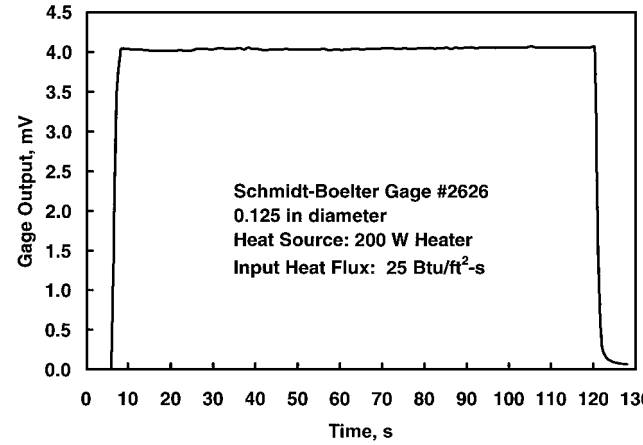

Fig. 8 Laboratory performance of test of a Schmidt–Boelter gauge.

Performance Testing

In an effort to determine the durability and other characteristics of the new gauges, investigators subjected them to the upper design point heat-flux inputs over relatively long run times in the ATMLab. The 200-W heater was the heat source used in these experiments. Figure 8 is a timewise record of the measured output of one of these gauges at a constant heat flux of about 25 Btu/(ft^2 · s) over a time duration of almost 2 min. The gauge exhibits a constant output over the entire test period. It is significant that these sensors, which were designed primarily for transient measurement applications, are capable of operation in quasi-steady-state applications. Other gauges were tested in basically the same manner with similar results. The purpose of this type of laboratory test was to evaluate the gauge performance for future applications in other test facilities.

Experimental Tests in Tunnel 9 and Tunnel B

Heat transfer gauge evaluation test programs were conducted in AEDC hypersonic Tunnels 9 and B in September 1998 and April 1999, respectively, to demonstrate the validity of the commonality of test measurement methodology using miniature fast-response Schmidt–Boelter gauges. The test model was a large (47 ± 0.05 in. length by 14 ± 0.05 in. diam) aluminum blunted sphere cone (7-deg half-angle) configuration. The model surface was polished to 32×10^{-6} in. mean roughness. As shown in Fig. 9, 10 AEDC 0.125-in.-diam Schmidt–Boelter gauges, 10 0.062-in.-diam Medtherm Corporation Schmidt–Boelter gauges, and 8 0.062-in.-diam coaxial surface thermocouples were installed in the aft section of the model. Several more coaxial thermocouples and several pressure gauges also were installed at locations on other forward sections of the cone model.

Tunnel 9 Test Program

Four runs were conducted in the Tunnel 9 test program, all at a nominal Mach number of 14 but at different Reynolds number test conditions. The first two runs were performed at high-Reynolds-number conditions (3.76×10^6/ft) with the model pitching at an APR of 36 deg/s. Nominal test conditions for Tunnel 9 run 2634 are

shown in Table 1. The initial position of the primary model axis was at a pitch angle of −6 deg with respect to the horizontal plane. A more detailed description of the Tunnel 9 test can be found in Ref. 18.

Figure 10 shows the timewise relative position of the primary axis of the test model in the Tunnel 9 Mach 14 hypersonic flow for run 2634. Note that the model is stationary in the wind tunnel from time 0.00 to about 0.80 s at an angle of −6 deg. The model is then pitched at an APR of about 36 deg/s until the end of the useful hypersonic flow test time. This occurs at a time of 1.45 s from the beginning of data acquisition. Therefore, the largest deviation of transient heating should begin at a time of about 0.80 s. This became apparent when the transient heating patterns on the test model were examined.

A good illustration of the transient nature of the heat-flux data obtained in Tunnel 9 is shown in Fig. 11. Timewise data from an AEDC Schmidt–Boelter gauge and a coaxial surface thermocouple located at nearby axial stations on the top ray 1 and bottom ray 3 of the model are shown together as the model is pitched upward at a rate of 36 deg/s. Data from the coaxial thermocouple (TC) are shown by the dashed line. Uncorrected data from the Schmidt–Boelter gauge are shown by the heavy solid line, and the corrected [see Eq. (9)] Schmidt–Boelter gauge data are shown by the lighter solid line. During the Tunnel 9 startup procedure from 0.00 to 0.80 s, the sensors on the top ray of the model are effectively the windward gauges because the primary axis of the model is located at an angle of −6 deg relative to the horizontal plane. During this time, these sensors experience relatively low laminar aerothermal heating, attaining levels of about 5 Btu/(ft^2 · s). However, as the model starts to pitch at a time of about 0.80 s, the aerothermal heating on the top ray of the model decreases at a fast rate. Measured data from the Schmidt–Boelter gauge A123 cannot keep up with data from the coaxial surface TC T121 (as shown in Fig. 11a). However, when the τ^* correction term is added to the measured heat flux, the data from the Schmidt–Boelter gauge track the coaxial TC data to good accuracy.

Conversely, the opposite effect is seen from the gauges on the bottom ray 3 of the model. During the tunnel startup procedures, these gauges experience insignificant heating as they are effectively on the leeward side because the primary axis of the model is located at a negative angle with the horizontal. However, as the model begins to pitch upward starting at about 0.80 s, these sensors become the windward gauges and begin to experience moderate aerothermal heating at levels of less than 10 Btu/(ft^2 · s) until a time just

Table 1 Nominal test conditions for Tunnel 9 run 2634

Parameter	Unit	Value	Uncertainty
Mach number	——	14.11	0.058
Pitot pressure	psia	11.44	0.026
*P*inf	psia	45×10^{-2}	3.81×10^{-4}
*T*inf	°R	92.9	0.439
rho	lb/ft^3	1.25×10^{-3}	8.51×10^{-6}
*U*inf	ft/s	6783	22.46
*Q*inf	psia	6.21	1.09×10^{-2}
Reynolds number	1/ft	3.51×10^{6}	2.01×10^{4}

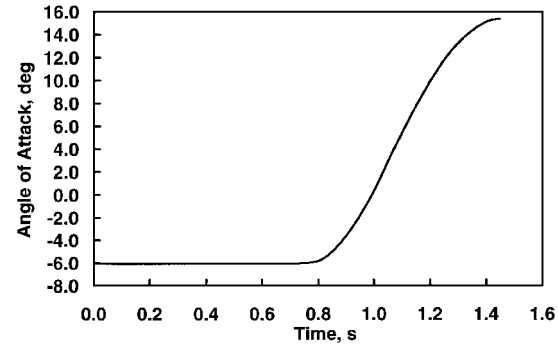

Fig. 10 Tunnel 9 run 2634 angle of attack vs time.

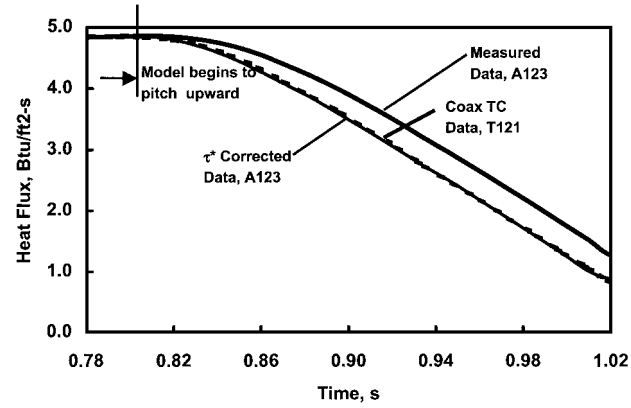

a) Ray 1 heat transfer data

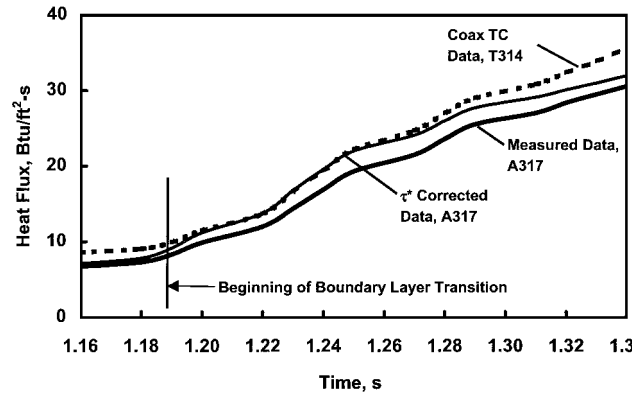

b) Ray 3 heat transfer data

Fig. 11 Tunnel 9 heat transfer data, run 2634.

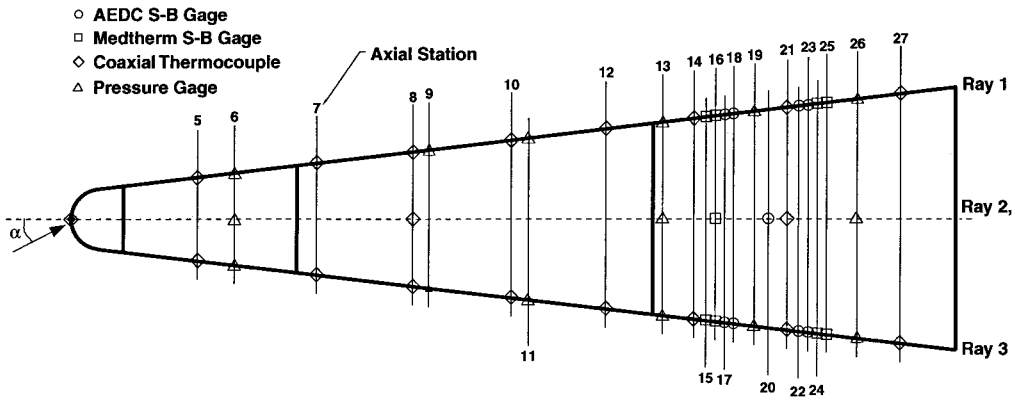

Fig. 9 Blunted sphere cone model.

before 1.20 s into the tunnel run. The heating on these gauges then increases quite rapidly with time for about 0.1 s before reaching levels approaching 40 Btu/(ft^2 · s). It is evident in this time period that the uncorrected data (heavy solid line) from the Schmidt–Boelter gauge lag the coaxial surface TC data (dashed line) by a significant amount. However, when the τ^* correction term is added to the uncorrected heat flux (lighter solid line) as shown by Eq. (9), there is good agreement between the coaxial TC and the Schmidt–Boelter gauge. It is speculated that the boundary layer transitions from laminar to turbulent starting at the aft end of the model configuration. It is the boundary-layer transition that drives the heat flux up so dramatically during this time period. Because the Schmidt–Boelter gauge A317 is located about 1.6 in. behind the coaxial TC T314, it is reasonable to believe that the Schmidt–Boelter gauge experiences transition before the coaxial TC. Therefore, the corrected data from the Schmidt–Boelter gauge appear to agree almost perfectly with the coaxial TC T314 for a short time. Then the data from these sensors approach their fully turbulent levels.

From the data shown in Fig. 11, it can be stated that the corrected Schmidt–Boelter gauge data track the coaxial TC data to good accuracy in highly transient heating environments. The advantage of obtaining simultaneous data from multiple Schmidt–Boelter gauges with the model pitching through an angle-of-attack range of 21 deg in a single run is great because fewer test runs are required (compared to the multiple fixed-attitude runs required before).

Tunnel B Test Program

As a further demonstration of the commonality of test measurement methodology approach between AEDC facilities, the Tunnel 9 blunt cone was run in the Hypersonic Wind Tunnel B at Mach 8 using a continuous-sweep mode of data acquisition. No changes or modifications to the model were performed; the fast-response Schmidt–Boelter gauges were simply connected to the Tunnel B data acquisition system, and the data reduction methodology of Ref. 19 was incorporated into the Tunnel B continuous-sweep data processing program. Because this was a quasi-steady-state measurement application, the coaxial surface TCs were not used. Traditionally, heat transfer data in AEDC Tunnel B have been acquired in a point-pause mode whereby the model attitude is set, the model is injected, and a single datapoint set is obtained for each run. Each model attitude requires a cool down and inject/retract cycle of several minutes, with the cool-down period being a function of tunnel conditions and model configuration. Using the current aerothermal sweep mode, investigators can obtain an entire range of pitch angles or roll angles during a single inject/retract/cool-down cycle. For the current test, pitch sweeps consisted of model polars from −6 to +14 deg with the data being reduced in 1-deg increments. The model pitch rate was 2.5 deg/s. A photograph of the blunt cone model installed in Tunnel B is shown in Fig. 12.

Presented in Figs. 13 and 14 are representative sweep results from run 12001 (laminar flow) and run 12006 (turbulent flow with boundary-layer trips), respectively, at a nominal angle-of-attack range of ±5 deg. Nominal test conditions for the two Tunnel B runs are shown in Table 2. The Tunnel B pitch rate of 2.5 deg/s results in an elapsed time of 4 s between the two sets of data at negative and positive angle of attack. The heat transfer data are shown in a sharp-cone similarity format where 1) X_s is the surface distance measured from the apex of a 7-deg sharp cone having a base diameter of 14 in. and 2) L_s is the corresponding surface distance from the apex to the base. As shown in Ref. 26, supersonic/hypersonic sharp-cone laminar flow heat transfer scales as the 0.5 power of surface distance, whereas for turbulent flow, the scaling parameter in terms of surface distance is 0.16. Note from Figs. 13 and 14 the agreement in measured heat transfer between ray 1 (wind) and ray 3 (lee) gauges at negative angle of attack, with ray 3 (wind) and ray 1 (lee) gauges at positive angle of attack. The ability of the Schmidt–Boelter gauges to measure accurately low heat-flux levels is demonstrated by the leeside laminar data in Fig. 13. The sharp-cone similarity format offers a reasonable way of collapsing the

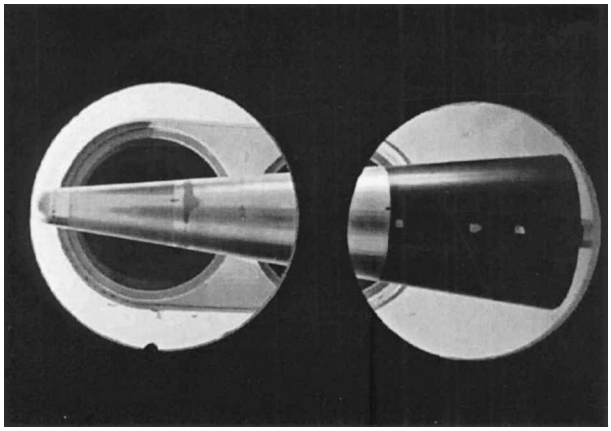

Fig. 12 Blunted sphere cone model in Tunnel B.

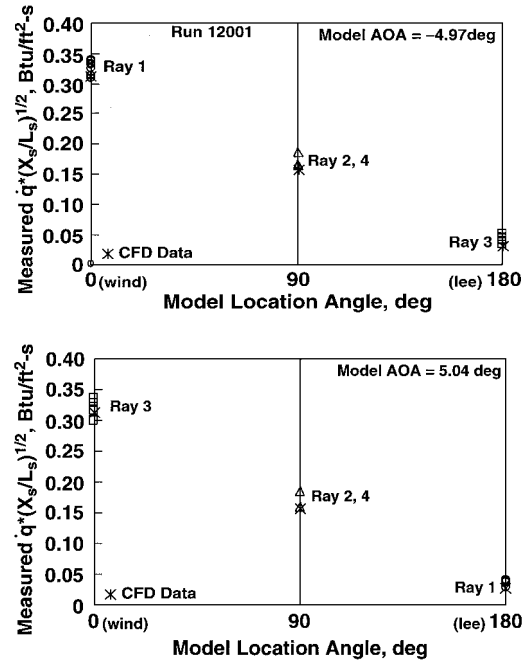

Fig. 13 Laminar sweep data for blunt cone in Tunnel B.

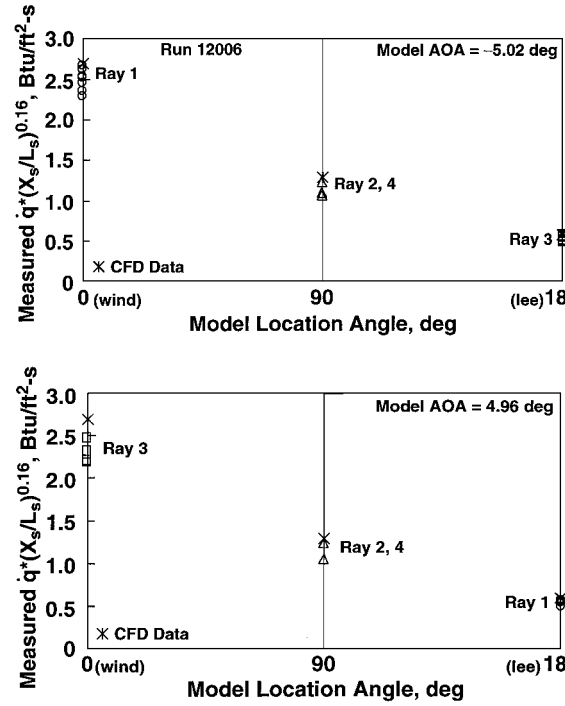

Fig. 14 Turbulent sweep data for blunt cone in Tunnel B.

Table 2 Tunnel B nominal test conditions and uncertainties

		Tunnel B run 12001		Tunnel B run 12006	
Parameter	Unit	Value	Uncertainty	Value	Uncertainty
Mach number	——	7.93	0.02	8.01	0.02
Total pressure	psia	190	0.08	800	0.32
Total temperature	°R	1209.7	4	13334.7	4
*P*inf	psia	2.05×10^{-2}	3.39×10^{-4}	8.17×10^{-2}	1.34×10^{-3}
*T*inf	°R	90.411	0.5976	98.7692	0.629
rho	lb/ft^3	1.90×10^{-5}	2.26×10^{-7}	6.94×10^{-5}	9.15×10^{-7}
*U*inf	ft/s	3696.59	6.19	3902.05	5.93
*Q*inf	psia	0.9004	0.0104	3.6685	0.0419
Reynolds number	1/ft	9.64×10^5	9.40×10^3	3.41×10^6	3.20×10^4

blunt cone data in terms of gauge surface location, typically within ±10%. For the laminar and turbulent cases, computational fluid dynamics (CFD) results are included within the data. These CFD data were computed using the parabolized Navier–Stokes TUFF/STUFF code described in Ref. 27. Because of the low pitch rate of the Tunnel B investigation, minimal transient corrections to the measured heat transfer rate determined by the methodology of Ref. 19 were required. These effectively uncorrected data are contrasted with the significant timewise data corrections that were required with the same gauges in the Tunnel 9 test program. In Tunnel B, the gauge response was essentially quasi steady state.

Uncertainty of AEDC Heat Transfer Measurements

The direct-reading heat-flux sensors described are calibrated in a wide-angle facility (quartz tube lamp bank[24]) against three NIST certified transfer standard conventional Schmidt–Boelter gauges. These transfer standards are calibrated at the NIST Optical Technology Division, Physics Laboratory in Gaithersburg, Maryland, on an annual basis. Calibrations of the transfer standards are traceable to electrical substitution radiometers[25] (ESRs). The typical total expanded uncertainty of a group of three AEDC transfer standard gauges is certified by NIST to be ±2% over a range of heat flux levels varying from 0.1 to 5 Btu/(ft$^2 \cdot$ s). Positioning of three transfer standard gauges with multiple gauges under calibration in a calibration block located under the lamp bank adds an uncertainty of ±1%. An experimental exercise performed in the early 1990s revealed the laboratory data acquisition system introduces an additional bias uncertainty of ±0.5%. The wind-tunnel facility data acquisition system has been experimentally determined to have an uncertainty of ±0.1% of full-scale reading. Therefore, the total estimated uncertainty of heat-flux measurements described here is less than ±4%. This uncertainty level is applicable across the heat transfer load range because no break point exists where uncertainty is observed to increase or decrease at a certain load level.

Conclusions

A new fast-response heat-flux sensor, based on a subtle variation of the conventional Schmidt–Boelter gauge concept used for several years in the AEDC continuous hypersonic wind tunnels has been developed and tested. The new sensor has time constants in the 10–15-ms range and near first-order time-response characteristics. Together with a recently developed general and easy-to-apply data reduction algorithm, a cost-effective commonality of heat transfer measurement methodology between AEDC Hypersonic Wind Tunnels B and C, and Tunnel 9 was developed. In addition, 200 of the new sensors were fabricated, characterized, and installed in a scale model of a complex flight vehicle and were successfully tested in Tunnel B in December 1999 at Mach numbers 6 and 8. Because the instrumentation is compatible with Tunnel 9 test requirements, the same model is essentially ready for a test program at higher Mach numbers without the expense of fabricating, calibrating, characterizing, and installing new gauges. The best case scenario would be to simply connect the gauges to the Tunnel 9 data acquisition system and conduct the test.

State-of-the-art FEA software with a transient heat transfer capability was extensively employed in the design of the new miniature (0.125-in.-diam) sensor. Results of the FEA analyses enabled the gauge designer to change physical dimensions and sensor materials to optimize the design for the required performance parameters. In addition, a perfectly general data reduction methodology used for experimental characterization of gauge response parameters and for easy implementation in transient-type measurement applications has been summarized. Finally, heat-transfer data obtained in a gauge evaluation test program for a cone model at Mach 8 in AEDC Tunnel B and at Mach 14 in Tunnel 9 were presented and found to be higher quality measurements that demonstrate the commonality of measurements in AEDC hypersonic wind tunnels.

Appendix: Selection of Fast-Response Schmidt–Boelter Gauge Response Time

From Eq. (9), the correction equation for fast-response Schmidt–Boelter gauge measured heat transfer is

$$\dot{q}_{\text{corr}} = \dot{q}_{\text{meas}} + \tau^* \left(\frac{\mathrm{d}\dot{q}_{\text{meas}}}{\mathrm{d}t} \right) \tag{A1}$$

with τ^* as the characteristic time measure of the integrated energy deficiency inherent in the gauge response. Equation (A1) is rearranged to form

$$\left(\frac{\dot{q}_{\text{corr}} - \dot{q}_{\text{meas}}}{\dot{q}_{\text{meas}}} \right) = \left(\frac{1}{\dot{q}_{\text{meas}}} \right) \left(\frac{\mathrm{d}\dot{q}_{\text{meas}}}{\mathrm{d}t} \right) \tau^* \tag{A2}$$

where the left-hand-side term represents the relative correction to the measured heat flux and the right-hand-side term represents the relative magnitude of the transient measured heat-flux gradient in time. Treating the right-hand-side term $(1/\dot{q}_{\text{meas}})\,(\mathrm{d}\dot{q}_{\text{meas}}/\mathrm{d}t)$ as a parameter, one can plot the left-hand-side term as a function of τ^* where values of 1–2 for $(1/\dot{q}_{\text{meas}})\,(\mathrm{d}\dot{q}_{\text{meas}}/\mathrm{d}t)$ are representative of transients in the AEDC Tunnel B and values of 4–8 for $(1/\dot{q}_{\text{meas}})\,(\mathrm{d}\dot{q}_{\text{meas}}/\mathrm{d}t)$ are representative of transients in AEDC Tunnel 9. Now the desired maximum relative correction to the measured heat flux that will yield a τ^* value corresponding to a chosen value of $(1/\dot{q}_{\text{meas}})\,(\mathrm{d}\dot{q}_{\text{meas}}/\mathrm{d}t)$ is selected. With τ^* thus determined, Eq. (8) gives the relationship between the gauge response time τ and the characteristic time measure of the integrated energy deficiency inherent in the gauge response τ^* as

$$\frac{\tau^*}{\tau} = \int_0^\infty \exp\left(\frac{-t}{\tau} \right)^n \mathrm{d}\left(\frac{t}{\tau} \right) = \left(\frac{1}{n} \right) \Gamma\left(\frac{1}{n} \right) \tag{A3}$$

which can be numerically evaluated in terms of the Gamma function Γ (no closed-form solution exists) for various values of the exponent n as shown in Fig. A1.

The data reduction methodology section of this paper describes how the gauge response characterization to a suddenly applied constant heat flux is used to determine the proper nonambiguous determination of n, with τ defined in the classical sense following Eq. (7):

$$g(t = \tau) = 1 - \exp(-1) \tag{A4}$$

where $g(t)$ is the quasi-first-order system response function defined by Eq. (6) as

$$g(t) = 1 - \exp(-t/\tau)^n \tag{A5}$$

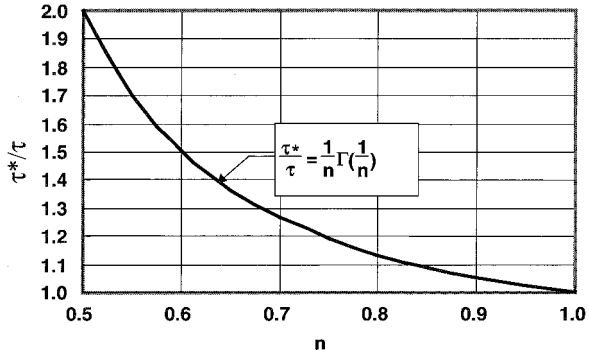

Fig. A1 Ratio of τ^* vs n.

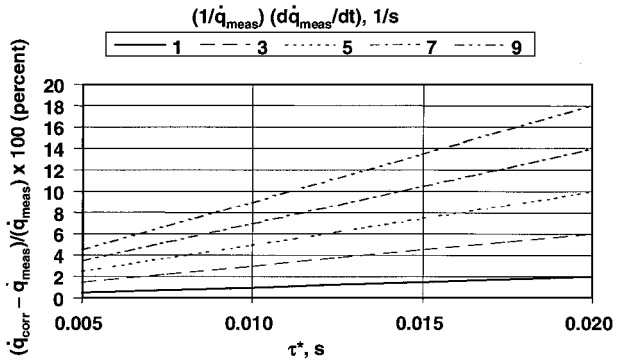

Fig. A2 Relative correction of measured heat flux vs τ^*.

For AEDC Schmidt–Boelter gauges having a heat sink, typical values of n range between 0.6 and 0.8; for AEDC Schmidt–Boelter gauges having a filler material, typical values of n range between 0.9 and 1.0. For a true first-order gauge response ($n \equiv 1.0$), then $\tau^* \equiv \tau$.

Example 1

For AEDC Tunnel 9 run 2570 blunt cone heat transfer, the maximum $(1/\dot{q}_{meas})\,(d\dot{q}_{meas}/dt)$ transient parameter is about 7/s. The desired maximum correction is 10%. From Fig. A2, $\tau^* \cong 0.014$ s. An AEDC heat sink Schmidt–Boelter gauge is to be used having an n exponent value of about 0.7. From Fig. A2, $\tau/\tau^* \cong 1.25$ for $n = 0.7$. Hence, the gauge should have a maximum time response τ of about $0.014/1.25 \cong 11$ ms for this application, yielding a desired maximum measured heat-flux correction of 10%. In general, the faster the gauge response is, the lower the correction amount to the measured heat flux.

Example 2

An AEDC filler material Schmidt–Boelter gauge having an exponent value of 0.9 and a time response τ of 14 ms is to be used for a transient heat transfer measurement application with a desired heat-flux correction of 6%. From Fig. A1, $\tau^*/\tau \cong 1.06$ for $n = 0.9$ so that $\tau^* = 0.015$ s for this application. From Fig. A2, the maximum $(1/\dot{q}_{meas})\,(d\dot{q}_{meas}/dt)$ transient parameter is about 4, corresponding to $\tau^* = 0.015$ s and a desired maximum heat-flux correction of 6%. In general, the faster the gauge response is, the larger the maximum $(1/\dot{q}_{meas})\,(d\dot{q}_{meas}/dt)$ parameter for a given desired measurement correction. Similarly, for a given gauge response, one must increase the maximum allowable heat-flux correction to accommodate larger transient parameters.

Acknowledgments

The authors gratefully acknowledge several people for their contributions to this work. Mark Felts, Annette Painter, and William Scott fabricated, calibrated, and characterized the Arnold Engineering Development Center (AEDC) Schmidt–Boelter gauges used in the AEDC wind-tunnel tests. James Thompson was the project engineer for the complex flight vehicle aerothermal tests and the blunt-cone gauge evaluation test at AEDC. Stuart Coulter wrote the program to characterize the time-response parameters for the AEDC Schmidt–Boelter gauges. Gregory Molvik obtained the computational fluid dynamics results for the cone model at the aerodynamic flow conditions experienced in the wind tunnel. The research reported herein was performed by the Arnold Engineering Development Center, Air Force Materiel Command. Work and analysis for this research were performed by personnel of Sverdrup Technology, Inc., AEDC Group, technical services contractor. Further reproduction is authorized to satisfy needs of the U.S. Government.

References

[1]Cook, W. J., and Felderman, E. J., "Reduction of Data from Thin-Film Heat-Transfer Gauges: A Concise Numerical Technique," *AIAA Journal*, Vol. 4, No. 3, 1966, pp. 561–566.

[2]Diller, T. E., and Kidd, C. T., "Evaluation of Numerical Methods for Determining Heat Flux with a Null-Point Calorimeter," *Proceedings of the 42nd International Instrumentation Symposium*, Instrument Society of America, Research Triangle Park, NC, 1996, pp. 251–262.

[3]Kidd, C. T., Nelson, C. G., and Scott, W.T., "Extraneous Thermoelectric EMF Effects Resulting from the Press-Fit Installation of Coaxial Surface Thermocouples in Metal Models," *Proceedings of the 40th International Instrumentation Symposium*, Instrument Society of America, Research Triangle Park, NC, 1994, pp. 317–335.

[4]Hedlund, E. R., Hill, J. A. F., Ragsdale, W. C., and Voisinet, R. L. P., "Heat Transfer Testing in the NSWC Hypervelocity Wind Tunnel Using Co-Axial Surface Thermocouples," U.S. Naval Surface Weapons Center, Rept. MP 80-151, Silver Spring, MD, March 1980.

[5]Kidd, C. T., "Recent Developments in High Heat-Flux Measurements at the AEDC," *Proceedings of the 36th International Instrumentation Symposium*, Instrument Society of America, 1990-Paper 90-156, Research Triangle Park, NC, May 1990, pp. 477–492.

[6]Miller, C. G., "Comparison of Thin-Film Resistance Heat-Transfer Gauges with Thin-Skin Transient Calorimeter Gauges in Conventional Hypersonic Wind Tunnels," NASA TM 83197, Dec. 1981.

[7]Wannenwetsch, G. D., Ticatch, L. A., Kidd, C. T., and Arterbury, R. L., "Measurements of Wing-Leading Edge Heating Rates on Wind Tunnel Models Using the Thin-Film Technique," AIAA Paper 85-0972, June 1985.

[8]Kidd, C. T., "High Heat-Flux Measurements and Experimental Calibrations/Characterizations," *The 1992 NASA Langley Measurement Technology Conference: Measurement Technology for Aerospace Applications in High-Temperature Environments*, edited by J. J. Singh and R. R. Antcliff, NASA CP-3161, 1992, pp. 31–50.

[9]"Method for Measuring Extreme Heat-Transfer Rates from High-Energy Environments Using a Transient, Null-Point Calorimeter," *Annual Book of ASTM Standards*, Vol. 15.03, Standard E 598-96, American Society of Testing and Materials, Philadelphia, 1997, p. 489.

[10]Merski, N. R., "Reduction and Analysis of Phosphor Thermography Data With the IHEAT Software Package," AIAA Paper 98-0712, Jan. 1998.

[11]Kidd, C. T., "Lateral Heat Conduction Effects on Heat-Transfer Measurements with the Thin-Skin Technique," *Instrument Society of America Transactions*, Vol. 26, No. 3, 1987, pp. 7–18.

[12]Trimmer, L. L., Matthews, R. K., and Buchanan, T. D., "Measurement of Aerodynamic Heat Rates at the AEDC von Karman Facility," International Congress on Instrumentation in Aerospace Simulation Facilities, 1973 Record, California Inst. of Technology, Pasadena, CA, Sept. 1973, pp. 35–44.

[13]Ledford, R. L., Smotherman, W. E., and Kidd, C. T., "Recent Developments in Heat-Transfer-Rate, Pressure, and Force Measurements for Hot-shot Tunnels," Arnold Engineering Development Center, AEDC TR-66-228 (AD-645764), Arnold AFB, TN, Jan. 1967.

[14]Gardon, R., "An Instrument for the Direct Measurement of Intense Thermal Radiation," *Review of Scientific Instruments*, Vol. 24, May 1953, pp. 366–370.

[15]Malone, E. W., "Design and Calibration of Thin-Foil Heat Flux Sensors," *Instrument Society of America Transactions*, Vol. 7, 1968, pp. 175–179.

[16]Kidd, C. T., "A Durable, Intermediate Temperature, Direct-Reading Heat-Flux Transducer for Measurements in Continuous Wind Tunnels," Arnold Engineering Development Center, AEDC TR-81-19 (AD-A107729), Arnold AFB, TN, Nov. 1981.

[17]Kidd, C. T., "How the Schmidt–Boelter Gauge Really Works," *Proceedings of the 41st International Instrumentation Symposium*, Instrument Society of America, Research Triangle Park, NC, 1995, pp. 347–368.

[18]Kidd, C. T., and Scott, W. T., "New Techniques for Transient Heat-Transfer Measurement in Hypersonic Flow at the AEDC," AIAA Paper 99-0823, Jan. 1999.

[19]Adams, J. C., Jr., and Kidd, C. T., "Data Reduction Methodology for Fast Response Schmidt–Boelter Heat-Transfer Gauges," *Proceedings of the ASME Heat Transfer Division—1999*, Vol. 4, HTD-Vol. 364-4, edited by

L. C. White, American Society of Mechanical Engineers, New York, 1999, pp. 57–64.

[20]Ragsdale, W. C., and Boyd, C. F., "Hypervelocity Wind Tunnel 9 Facility Handbook, Third Edition," U.S. Naval Surface Weapons Center, TR 91-616, Silver Spring, MD, July 1993.

[21]Terrell, J. P., Hager, J. M., Onishi, S., and Diller, T. E., "Heat Flux Microsensor Measurements and Calibrations," *The 1992 NASA Langley Measurement Technology Conference: Measurement Technology for Aerospace Applications in High-Temperature Environments*, edited by J. J. Singh and R. R. Antcliff, NASA CP-3161, 1992, pp. 69–80.

[22]MSC/NASTRAN for Windows, Ver. 3.0, Command Reference Guide, Release Guide, MacNeal–Schwendler Corp., Los Angeles, Oct. 1997.

[23]Hudson, D. J., "Analysis of Data Reduction Procedures for Schmidt–Boelter Heat Transfer Gauges for Use in NSWC Tunnel 9," Science Applications International Corp., Memorandum, Valley Forge, PA, Aug. 1997.

[24]Kidd, C. T., "Determination of the Uncertainty of Experimental Heat-Flux Calibrations," Arnold Engineering Development Center, AEDC TR-81-19 (AD-A107729), Arnold AFB, TN, Nov. 1981.

[25]Murthy, A. V., Tsai, B. K., and Saunders, R. D., "Radiative Calibration of Heat Flux Sensors at NIST—An Overview," *Proceedings of the ASME Heat Transfer Division—1997*, Vol. 3, HTD-Vol-353-3, American Society of Mechanical Engineers, New York, 1997, pp. 159–164.

[26]Boylan, D. E., "A Direct Comparison of Reentry F Heat-Transfer-Rate Data to Ground Facility Measurements," Arnold Engineering Development Center, AEDC TR-74-107 (AD-C000236), Arnold AFB, TN, Dec. 1974.

[27]Molvik, G. A., and Merkle, C. L., "A Set of Strongly Coupled, Upwind Algorithms for Computing Flows in Chemical Nonequilibrium," AIAA Paper 89-0199, Jan. 1989.

M. Torres
Associate Editor